Multiphoton entanglement engineering via projective measurements

Christian Schmid[a,b], Nikolai Kiesel[a,b], Witlef Wieczorek[a,b], Reinhold Pohlner[a,b] and Harald Weinfurter[a,b]

[a]Max-Planck-Institut für Quantenoptik, Hans-Kopfermann-Strasse 1, D-85748 Garching, Germany;

[b]Department für Physik, Ludwig-Maximilians-Universität, D-80797 München, Germany;

ABSTRACT

We present strategies to obtain different classes of three and four photon entangled symmetric states from a single experimental setup. The basic idea originates from the property of the symmetric Dicke state with two excitations to connect the two inequivalent types of genuine tripartite entanglement. We experimentally confirm the distinct types of entanglement of the observed states. We further propose an extension of the applied scheme that allows one to obtain different classes of four-photon entanglement by adding a fifth photon. The requirement of a single fifth photon is currently a technical challenge, and thus we consider the approach of using a strongly attenuated weak coherent beam instead.

Keywords: Entanglement, spontaneous parametric down conversion, entanglement classification, linear optics

1. INTRODUCTION

Entanglement plays a central role in the field of quantum information. While entanglement in bipartite systems is well understood, the generalization to more than two parties is not straightforward. The reason is that in the multipartite case different types of entanglement exist. Recently, the equivalence of quantum states under stochastic local operations and classical communications (SLOCC) was successfully used as one possible classification of multiparty entanglement.[1–4] It is particularly relevant for evaluating the usefulness of states for multiparty quantum communication: States of the same SLOCC-class can be used for the same applications. While for tripartite systems there are only two different classes of genuine tripartite entanglement,[2] the structure is richer for four qubits.[3,5]

Experimentally, several particularly interesting quantum states have been studied in various physical systems. So far, the biggest variety of states was observed in experiments that rely on photonic qubits.[6–10] There, the information is encoded in the polarization of single photons propagating in well-defined spatial modes. These photons are usually produced by spontaneous parametric down conversion and further processed by a simple linear optics network in combination with conditional detection. Typically for such setups, the design of the optical network is especially tailored to the particular state that should be observed. Consequently, once a particular network is built it will not offer flexibility on the choice of state. The flexibility to gain any entangled state within a single configuration is theoretically possible by a commensurate amount of linear optics quantum logic including non-local gate operations. To date, this solution is however technically restricted by the efficiency of the setups. The major problem in this regard is the probabilistic success of the required linear optics quantum gates which adds to the probabilistic nature of the photon source as well as the probabilistic photon detection process. Altogether this would inevitably lead to unreasonably long data acquisition times. Here, we present a strategy to observe a variety of different entangled states with just *one* linear optics setup that does not rely on universal quantum gates. It is rather based on the property of certain entangled states which connect different kinds of entanglement of a lower qubit number. That means our approach aims at a simple setup for the observation of a (n+1)-qubit state that can be reduced by different local measurements to n-qubit states of different SLOCC-classes.

Send correspondence to Christian Schmid, E-mail: Christian.Schmid@mpq.mpg.de

Quantum Communications Realized
edited by Yasuhiko Arakawa, Masahide Sasaki, Hideyuki Sotobayashi,
Proc. of SPIE Vol. 6780, 67800E, (2007) · 0277-786X/07/$18 · doi: 10.1117/12.734697

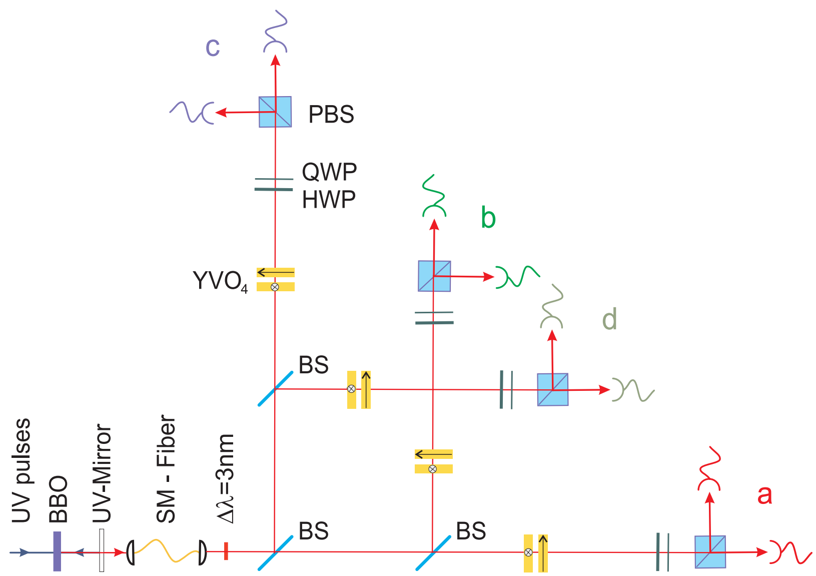

Figure 1. Experimental setup for the observation and analysis of the four-photon polarization-entangled state $|D_4^{(2)}\rangle$, observed after the symmetric distribution of four photons onto the spatial modes a,b,c and d via non-polarizing beam splitters. The photons are obtained from type-II collinear spontaneous parametric down conversion (SPDC) in a 2 mm β-Barium Borate (BBO) crystal pumped by 600 mW UV-pulses. The phases between the four output modes are set via pairs of birefringent Yttrium-Vanadate-crystals (YVO_4). Half and quarter wave plates (HWP, QWP) together with polarizing beam splitters (PBS) are used for the polarization analysis.

We begin our investigations first with three qubit states that can be obtained from a four qubit resource state. It turns out that the symmetric Dicke state with two excitations represents such a resource.[11] Via a simple projective measurement on a single qubit one can obtain the three-photon W_3 state and the G_3 state[12] which is GHZ_3 class, i.e. can be transformed to a GHZ_3 state via stochastic local operations only, as we will show. Second, we propose how the setup, used for the observation of the Dicke state, can be easily extended to yield a five qubit resource state. Based on this a big variety of different four qubit entangled states can be obtained by a clever combination of a local single qubit operation and projective measurement. Prominent examples of resulting states are the GHZ_4 and W_4 (as well as the symmetric Dicke state with two excitations itself). Finally, we discuss technical challenges of the proposed extension scheme and show first experimental steps towards a realization.

2. SYMMETRIC THREE-PHOTON ENTANGLED STATES OBTAINED THROUGH A SINGLE PROJECTION MEASUREMENT

With the aim of engineering multi-photon entanglement by a single projective measurement we start with the description of the state that accomplishes this task for three qubits: The four qubit symmetric Dicke state with two excitations $|D_4^{(2)}\rangle$.

2.1. Four-photon resource state

Generally, a symmetric N-qubit Dicke state[13,14] with M excitations is the equally weighted superposition of all permutations of N-qubit product states with M vertically polarized photons and $(N-M)$ horizontally polarized photons, here denoted by $|D_N^{(M)}\rangle$. Hence for $N=4$ and $M=2$ we get:

$$|D_4^{(2)}\rangle = \frac{1}{\sqrt{6}}(|HHVV\rangle + |HVHV\rangle + |VHHV\rangle + |HVVH\rangle + |VHVH\rangle + |VVHH\rangle) \quad (1)$$

with, e.g., $|VVHH\rangle = |V\rangle_a \otimes |V\rangle_b \otimes |H\rangle_c \otimes |H\rangle_d$, where $|H\rangle$ and $|V\rangle$ denote linear horizontal (H) and vertical (V) polarization of a photon in the spatial modes (a, b, c, d) (Fig. 1). Evidently, this is a superposition of the six possibilities to distribute two horizontally and two vertically polarized photons into four modes. Accordingly, in order to observe this state experimentally, we create four indistinguishable photons with appropriate polarizations in one spatial mode and distribute them with polarization independent beam splitters (BS) (Fig. 1).[11, 15]

As source of the four photons we use the second order emission of collinear type II spontaneous parametric down conversion (SPDC). UV pulses with a central wavelength of 390 nm and an average power of about 600 mW from a frequency-doubled mode-locked Ti:Sapphire laser (pulse length ≈130 fs) are used to pump a 2 mm thick BBO (β-Barium Borate, type-II) crystal. This results in two horizontally and two vertically polarized photons. Dichroic UV-mirrors serve to separate the UV-pump beam from the down conversion emission. A half wave plate together with a 1 mm thick BBO crystal compensates walk-off effects (not shown in Fig. 1). Coupling the four photons into a single mode fiber exactly defines the spatial mode. The spectral selection is achieved with a narrow bandwidth interference filter ($\Delta\lambda = 3$ nm) at the output of the fiber. Birefringence in the non-polarizing beam splitter cubes (BS) is compensated with pairs of perpendicularly oriented 200 μm thick birefringent Yttrium-Vanadate crystals (YVO_4) in each of the four modes. Altogether, the setup is stable over several days which is mainly limited by misalignment effects in the pump laser system affecting rather the count rate than the quality of the state.

For the characterization of the state polarization analysis is performed in all of the four outputs. For each mode we choose the analysis direction with half (HWP) and quarter wave plates (QWP) and detect the photons with the corresponding orthogonal polarizations in the outputs of polarizing beam splitters using single photon detectors (Si-APD). The detected signals are fed into a multi-channel coincidence unit which allows to simultaneously register any possible coincidence between the inputs. The rates for each of the 16 characteristic four-fold coincidences were corrected for the different detection efficiencies in each polarization analysis.

A count rate of 60 four-fold coincidences per minute was obtained what allows the accomplishment of a complete state tomography. The experimental state shows a fidelity of $\mathcal{F}_{\text{exp}} = 0.844 \pm 0.008$. To test whether we indeed observe genuine four-partite entanglement we use the generic form of the witness operator $\mathcal{W}_{\text{g}}^{D_4^{(2)}} = \frac{2}{3}\mathbb{1} - |D_4^{(2)}\rangle\langle D_4^{(2)}|$.[16] The corresponding expectation value depends directly on the observed fidelity: $\text{Tr}[\mathcal{W}_{\text{g}}^{D_4^{(2)}} \rho_{\text{exp}}] = \frac{2}{3} - F_{\text{exp}} = -0.177 \pm 0.008$ and is positive for all biseparable states. Thus, the observed state is genuinely four-partite entangled.

2.2. Projected three-photon entangled states

The claim that the above source of four-photon entanglement offers the possibility to obtain different types of three-photon entangled states by a local measurement on a single qubit is not trivial and not possible for every four-photon entangled state: For example, a projective measurement on the state $|GHZ_4\rangle$[17, 18] and $|C_4\rangle$[9, 10] can either still render tripartite GHZ_3 like entanglement or become (partly) separable. That holds equivalently for the state $|W_4\rangle$ (or $|D_4^{(1)}\rangle$ in the present notation), but the tripartite entanglement will always be W_3 type. In the following we will demonstrate what is, in contrast, expected for $|D_4^{(2)}\rangle$.

2.2.1. The three-photon entangled W_3 state

Let us start with a projective measurement in the computational basis on the photon in mode d. Due to the symmetry of $|D_4^{(2)}\rangle$ the result is independent of the chosen photon.

$$ {}_d\langle V | D_4^{(2)}\rangle = |W_3\rangle = \frac{1}{\sqrt{3}}(|HHV\rangle + |HVH\rangle + |VHH\rangle), \quad (2) $$

$$ {}_d\langle H | D_4^{(2)}\rangle = |\overline{W}_3\rangle = \frac{1}{\sqrt{3}}(|HVV\rangle + |VHV\rangle + |VVH\rangle). \quad (3) $$

As the two states are equivalent up to a spin flip, this shows that a W_3 state is obtained with certainty independent of the measurement result.

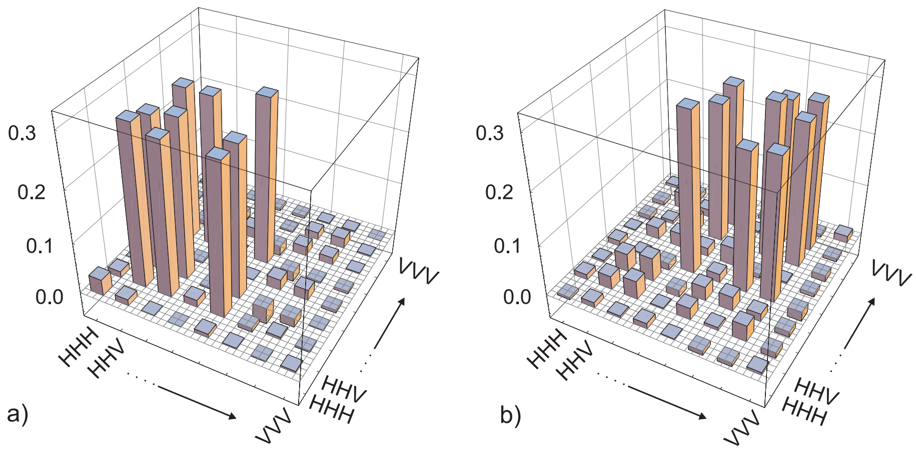

Figure 2. Real parts of density matrices for the W_3 states after projection of photon d onto $|V\rangle$ (a) and $|H\rangle$ (b). The imaginary parts consist of noise only, comparable to the noise in the real part.

In figure 2, the density matrices, ρ_{W_3} and $\rho_{\overline{W}_3}$, obtained for the corresponding measurements are shown. Clearly visible are the three W_3-characteristic terms with their coherences. The noise of the real and imaginary parts are comparable. The states are obtained with a fidelity of $\mathcal{F}_{W_3} = 0.882 \pm 0.015$ and $F_{\overline{W}_3} = 0.835 \pm 0.015$. To test whether the observed states are indeed tripartite entangled we employ the generic entanglement witness for W_3 states:

$$\mathcal{W}_g^{W_3} = \frac{2}{3}\mathbb{1} - |W_3\rangle\langle W_3| \tag{4}$$

The same entanglement witness is valid for $|\overline{W}_3\rangle$ when the corresponding projector is used. With the above fidelities we find: $\mathrm{Tr}[\mathcal{W}_g^{W_3}\rho_{W_3}] = -0.215 \pm 0.015$ and $\mathrm{Tr}[\mathcal{W}_g^{\overline{W}_3}\rho_{\overline{W}_3}] = -0.168 \pm 0.015$, where the negative values prove presence of genuine tripartite entanglement.

2.2.2. The three-photon G_3 state

For projective measurements in bases that are conjugate to the computational one we observe G_3 states, which are superpositions of a W_3 state and its spin-flipped counterpart. For example for a measurement in mode d in the $\pm 45\,^\circ$-basis (with $|\pm\rangle = 1/\sqrt{2}(|H\rangle \pm |V\rangle)$) we get:

$$_d\langle \pm | D_4^{(2)}\rangle = \frac{1}{\sqrt{2}}(|\overline{W}_3\rangle \pm |W_3\rangle) = |G_3^{\pm}\rangle \tag{5}$$

$$= \frac{1}{\sqrt{6}}(|HVV\rangle + |VHV\rangle + |VVH\rangle \pm |HHV\rangle \pm |HVH\rangle \pm |VHH\rangle). \tag{6}$$

Such states are not only genuinely tripartite entangled. In contrast to the previously observed W_3 states they are GHZ_3-class states. That means they cannot be converted into W_3 states by stochastic local operations and classical communication (SLOCC). Thus, the state $|D_4^{(2)}\rangle$ allows to obtain two truely different types of tripartite entangled quantum states.

As these G_3 states belong to the GHZ_3 class, it is possible to transform them via SLOCC operations to the three-photon GHZ_3 state. The relation can be calculated explicitly, here exemplarily for the G_3^- state:

$$(\mathcal{H}\otimes\mathcal{H}\otimes\mathcal{H})(\mathcal{T}_+\otimes\mathcal{T}_+\otimes\mathcal{T}_+)(\mathcal{H}\otimes\mathcal{H}\otimes\mathcal{H}) \quad |G_3^-\rangle = \frac{1}{3}|GHZ_3\rangle, \tag{7}$$

$$(\mathcal{H}\otimes\mathcal{H}\otimes\mathcal{H})(\mathcal{T}_-\otimes\mathcal{T}_-\otimes\mathcal{T}_-)(\mathcal{H}\otimes\mathcal{H}\otimes\mathcal{H}) \quad |GHZ_3\rangle = \frac{1}{\sqrt{3}}|G_3^-\rangle, \tag{8}$$

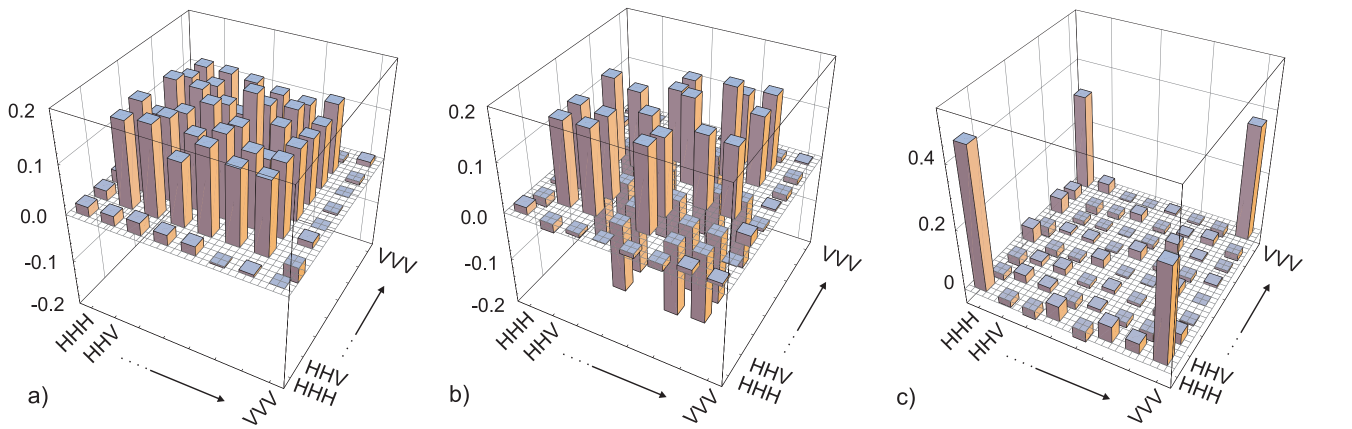

Figure 3. Real parts of density matrices for G_3 states after projection of photon d onto $|+\rangle$ (a) and $|-\rangle$ (b). In (c), the real part of the (calculated) density matrix when the state after projection on $|-\rangle$ is transformed by $(\mathcal{H}\mathcal{T}_+\mathcal{H})^{\otimes 3}$ is shown, clearly exhibiting the structure of a GHZ_3 state. All imaginary parts consist of noise only, comparable to the noise in the real part.

with $\mathcal{T}_\pm = \frac{(\pm 1)^{1/6}}{2}((\frac{1}{\sqrt{3}}+i)\cdot\hat{\sigma}_x + i(\frac{1}{\sqrt{3}}-i)\cdot\hat{\sigma}_y)$ and $\mathcal{H}$ is the Hadamard transformation. These stochastic local operations (no classical communication necessary) can straightforwardly be implemented via wave plates and a polarization dependent beam splitter with a perfect transmission for vertical and 1/3 transmission for horizontal polarization. This kind of beam splitter is commercially available and was already successfully used for the implementation of linear optics phase gates.[19–21]

In figure 3a) and b), the density matrices, $\rho_{G_3^+}$ and $\rho_{G_3^-}$, of the experimentally obtained G_3 states are displayed. They show fidelities of $\mathcal{F}_{G_3^+} = 0.875 \pm 0.016$ and $\mathcal{F}_{G_3^-} = 0.897 \pm 0.019$ to the ideal states.

Knowing that G_3 states are GHZ_3 class in the ideal case, we still need to verify this result in the experiment, where noise reduces the quality of the states. To this end, we apply the transformation $(\mathcal{H}\mathcal{T}_+\mathcal{H})^{\otimes 3}$ exemplarily to one of the experimentally observed states ($\rho_{G_3^-}$). The real part of the resulting density matrix ρ_{GHZ_3} is shown in figure 3 c), where the structure of a GHZ_3 state is clearly visible. The fidelity to the corresponding GHZ_3 state is $\mathcal{F}_{GHZ_3} = 0.733 \pm 0.024$. As the applied transformation is a stochastic *local* operation, the resulting state belongs still to the same entanglement class as the original one. Thus, we can apply the GHZ_3 generic entanglement witness to test the state's entanglement. The witness is:

$$\mathcal{W}^{\alpha}_{GHZ_3} = \alpha\mathbb{1} - |GHZ_3\rangle\langle GHZ_3|\,. \tag{9}$$

This entanglement witness detects genuine tripartite entanglement for $\alpha = 0.5$ and GHZ_3-type entanglement for $\alpha = 0.75$. Experimentally, we find $\mathrm{Tr}\left[\mathcal{W}^{0.5}_{GHZ_3}\,\rho_{GHZ_3}\right] = -0.233 \pm 0.024$, which clearly proves the genuine tripartite entanglement in ρ_{GHZ_3} and therefore in the original G_3^- state. The witness for GHZ_3-type entanglement $\mathrm{Tr}\left[\mathcal{W}^{0.75}_{GHZ_3}\,\rho_{GHZ_3}\right] = 0.017 \pm 0.024$, however, has a slightly positive expectation value and therefore gives no conclusive result on the type of genuine tripartite entanglement observed in the state.

As another test of GHZ_3 type entanglement, we can use optimized local filtering operations $\widehat{F} = A \otimes B \otimes C$ acting on the generic GHZ_3-witness.[22,23] The resulting witness operator is then $\mathcal{W}' = \widehat{F}^\dagger \mathcal{W}_{GHZ_3} \widehat{F}$. Here A, B and C are 2×2 complex matrices determined through numerical optimization to find the optimal witness for the detected state. In the measurement, GHZ_3 type entanglement is indeed detected with an expectation value of $\mathrm{Tr}[\rho_{G_3^-}\mathcal{W}'] = -0.029 \pm 0.023$ proving that the observed state is *not* W_3 class.

3. EXTENSION TO SYMMETRIC FOUR PHOTON ENTANGLED STATES

We have seen that the symmetric Dicke state with two excitations enables access to distinct classes of genuine tripartite entanglement. Via local operations this is absolutely impossible within the space of three qubits and

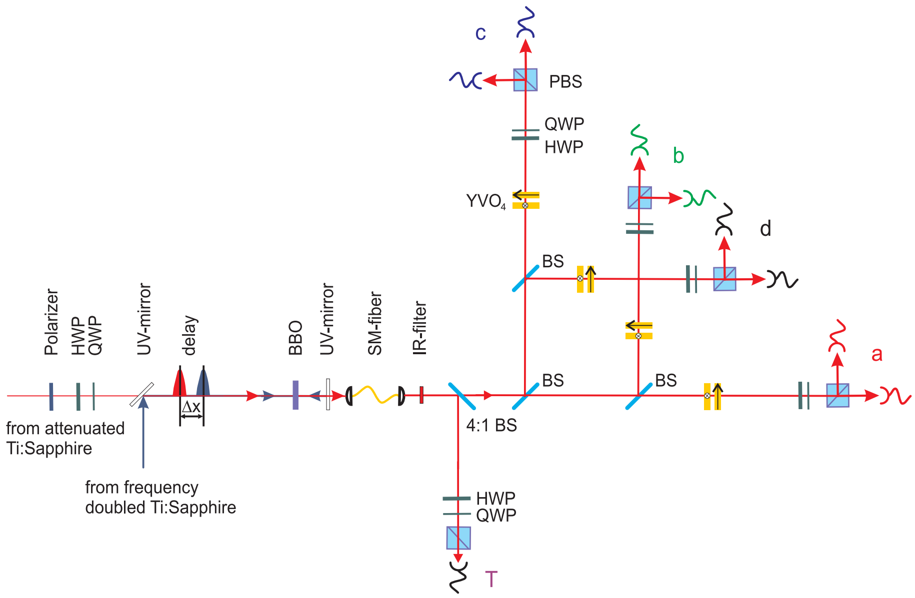

Figure 4. Experimental setup for the observation of a variety of symmetric four-photon entangled states. The setup shown in figure 1 is extended by feeding an additional single photon collinearly and coincidentally with the UV pump beam into the SPDC crystal. By conditional detection we can split a single photon into the trigger mode T on a polarization independent 4:1 beam splitter and project it on an arbitrary polarization. The state obtained after distributing the other four photons onto spatial modes a, b, c, d differs fundamentally in dependence on the polarization of the input photon and the projective trigger measurement.

even not achievable by entanglement catalysis either.[24] However, with proper entanglement of a higher qubit number as resource, (in our case just one qubit overhead), the task could be accomplished. In the following we will extend this idea to five-photon states and investigate, which different four-photon entanglement classes are accessible.

3.1. Five-photon resource state and projected four-photon entangled states

The state $|D_4^{(2)}\rangle$ was obtained by the symmetric distribution of two horizontally and two vertically polarized photons. The straightforward approach to obtain five-photon Dicke states is to add a fifth photon to the same spatial mode and then distribute all photons symmetrically onto five modes. The state emitted by the second order SPDC before the photons are split up is $a_{\mathrm{V}}^{\dagger^2} a_{\mathrm{H}}^{\dagger^2} |0\rangle$, where $|0\rangle$ is the vacuum state and $a_i^\dagger$ is the creation operator of a photon with polarization $i \in \{H, V\}$. By adding a fifth photon with arbitrary polarization $\alpha a_{\mathrm{H}}^\dagger + \beta e^{i\phi} a_{\mathrm{V}}^\dagger$ we get the state $\left[\alpha(a_{\mathrm{V}}^{\dagger^2} a_{\mathrm{H}}^{\dagger^3}) + \beta e^{i\phi}(a_{\mathrm{V}}^{\dagger^3} a_{\mathrm{H}}^{\dagger^2})\right] |0\rangle$, where all parameters are real and $\alpha^2 + \beta^2 = 1$. When distributing these photons symmetrically onto five spatial modes analogous to the state $|D_4^{(2)}\rangle$, this obviously results in superpositions of Dicke states: $|\psi_5\rangle = \alpha |D_5^{(2)}\rangle + \beta e^{i\phi} |D_5^{(3)}\rangle$. However, here we are interested in four-photon states that are obtained after a single projective measurement on one of the five photons. Under the condition of detecting a single photon with arbitrary polarization, corresponding to the application of an annihilation operator $\overline{\alpha} a_H + \overline{\beta} e^{-i\overline{\phi}} a_V$, a four-photon state is created. Thus, starting from the five-photon state before a symmetric distribution, the set of four-photon states we can obtain with this operation is:

$$\left[\alpha\overline{\beta} e^{-i\overline{\phi}} (a_{\mathrm{V}}^\dagger a_{\mathrm{H}}^{\dagger^3}) + \overline{\alpha}\beta e^{i\phi} (a_{\mathrm{V}}^{\dagger^3} a_{\mathrm{H}}^\dagger) + (\alpha\overline{\alpha} + \beta\overline{\beta} e^{i(\phi - \overline{\phi})})(a_{\mathrm{V}}^{\dagger^2} a_{\mathrm{H}}^{\dagger^2})\right] |0\rangle. \quad (10)$$

Now, a symmetric distribution of these four photons onto four modes yields the states:

$$|\psi\rangle = \alpha\overline{\beta} e^{-i\overline{\phi}} |D_4^{(1)}\rangle + \overline{\alpha}\beta e^{i\phi} |D_4^{(3)}\rangle + (\alpha\overline{\alpha} + \beta\overline{\beta} e^{i(\phi - \overline{\phi})}) |D_4^{(2)}\rangle. \quad (11)$$

Thus, we obtain superpositions of the three entangled symmetric Dicke states of four photons.

These states are members of very different SLOCC entanglement classes.[3, 5] Let us shortly take a closer look at three particularly interesting cases. First, it is obvious that one can obtain the state $|D_4^{(2)}\rangle$ when following the lines of the presented method. We can add either a horizontally or a vertically polarized photon and project onto the same polarization in order to obtain $|D_4^{(2)}\rangle$. This corresponds to the case where the coefficients of $|D_4^{(1)}\rangle$ and $|D_4^{(3)}\rangle$ vanish. Either of the latter states corresponds to the well known W_4 state.[2] They are obtained with this method when either a horizontally or a vertically polarized photon is added and the orthogonal one is projected. The most surprising fact is that we can even obtain a four-photon GHZ_4 state: $|GHZ_4^-\rangle = 1/\sqrt{2}(|HHHH\rangle - |VVVV\rangle)$. This is most easily seen when the GHZ_4^- state is rewritten in the following form:

$$(\mathcal{H}\otimes\mathcal{H}\otimes\mathcal{H}\otimes\mathcal{H})\,|GHZ_4^-\rangle = \frac{1}{\sqrt{2}}(|D_4^{(1)}\rangle + |D_4^{(3)}\rangle). \tag{12}$$

It can be easily calculated that the state on the right hand side is obtained in our scheme for addition of a left circularly polarized photon and a projection measurement on its orthogonal polarization, i.e. right circular polarization, or vice versa. In general, the condition that the amplitude of $|D_4^{(2)}\rangle$ vanishes corresponds exactly to the case of orthogonality between the added and projected photon. Thus, a direct transition between GHZ_4^- and W_4 states can be obtained.

3.2. First experimental steps

One possibility to add an additional photon to the four-photon emission of the SPDC is the overlap of the five photons on a beam splitter. As the photons go only probabilistically to the same spatial mode, this approach is rather inefficient. Here, we propose the overlap of the additional photon with the SPDC photons directly in the BBO crystal. This has several advantages. The alignment of the setup is simplified as the transversal distinguishability of the photon modes is filtered by coupling all photons in the same single mode fiber. Also, we even increase the number of observable five-photon coincidences as the SPDC emission is stimulated by the presence of the additional photon. A corresponding setup for this experimental approach is shown in figure 4. Ideally, the added photon originates from a single photon source matching perfectly the SPDC photons, i.e. it should be indistinguishable in temporal, spatial and spectral modes. As perfect single photon sources with these requirements are still not available we take the approach of adding photons from a pulsed weak coherent beam (WCB).[25] This implies several experimental challenges, due to the Poissonian photon number statistics of a coherent light source. Firstly, as not only single but also multiple photons are found in single pulses, the beam has to be sufficiently attenuated. That leads to a trade off between total count rate and multiple photon noise. Secondly, at a first glance the coherent overlap between the photons of the two sources in the BBO crystal could be thought of as second order interference. This would require a stabilization of the optical path lengths on the order of the coherence length of the used photons, i.e. on μm scale, what can be achieved with minor effort. However, a closer look reveals that also first order interference occurs due to multiple photons in the WCB. This interference happens between the different possibilities to obtain certain coincidence detection events. For example, a three-photon coincidence detection event might be caused by two photons emitted by the SPDC and one by the WCB or zero by the SPDC and three by the WCB. These possibilities are indistinguishable for particular polarization settings and would differ randomly in phase due to fluctuations in the optical path lengths on the order of the photons' wavelength. Hence, in contrast to the first intuition, the optical path lengths in the experimental setup need to be stabilized on the sub-μm scale, what requires active control.

The weak coherent beam is derived from the Ti:Sapphire laser that also pumps after frequency doubling the BBO crystal for the SPDC emission. It is collinearly fed to the SPDC emission as depicted in figure 4 and coupled in the same single mode fiber ensuring spatial mode matching. Spectral indistinguishability is achieved by a 3 nm interference filter at the output of the single mode fiber. Temporal overlap is adjustable by a delay line in the weak coherent beam. Any desired input polarization of the added photon is set by a polarizer followed by a half and quarter wave plate. Hence, at the output of the single mode fiber behind the interference filter we have five indistinguishable photons with different polarization. The measurement aimed at the state reduction is achieved by extracting one of the photons with a 4:1 beam splitter to the trigger mode T and projecting it onto any desired polarization. The remaining four photons are distributed symmetrically onto four spatial modes a, b, c, d analogously to the experimental setup for the observation of $|D_4^{(2)}\rangle$.

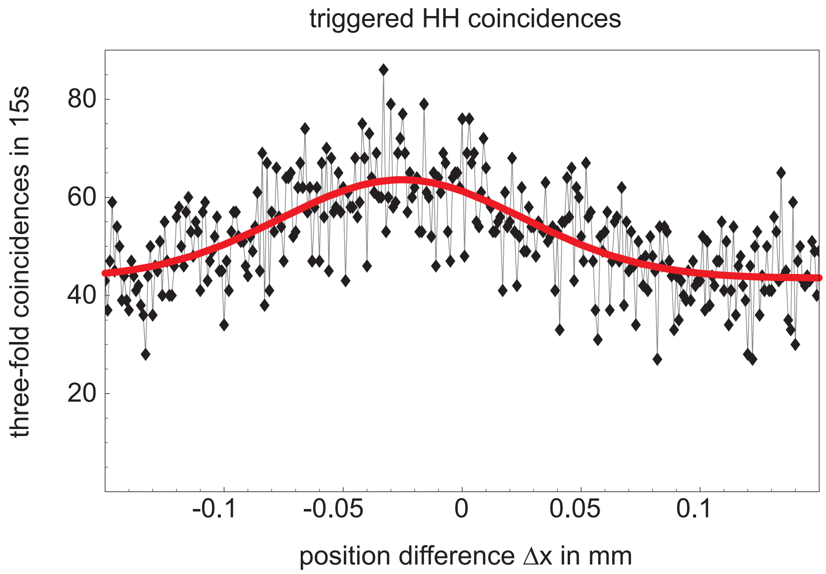

Figure 5. Three-fold coincidences between modes a and c when detecting horizontally polarized photons triggered onto the detection of a right circularly polarized photon in mode T. The temporal overlap between the weak coherent beam with left circular polarization and the SPDC emission is changed by adjusting the relative position Δx between the two pulses. The increase in count rate indicates the coherence between both sources.

To demonstrate the principle feasibility of this approach we discuss the observation of a triggered two photon state, i.e. a three-photon detection stemming from the added photon and the first order emission of the SPDC. Without an additional photon the symmetric distribution of the SPDC yields the state $|\psi^+\rangle = 1/\sqrt{2}(|HV\rangle + |VH\rangle)$. When we add a left circularly polarized photon and trigger onto its orthogonal polarization, i.e. right circular, a coherent overlap of both sources results in the triggered state $|\phi^+\rangle = 1/\sqrt{2}(|RL\rangle + |LR\rangle) = i/\sqrt{2}(|HH\rangle + |VV\rangle)$, where $|R/L\rangle = 1/\sqrt{2}(|H\rangle \pm i|V\rangle)$. An incoherent overlap will, however, give the mixed state $\rho = 1/2(|RL\rangle\langle RL| + |LR\rangle\langle LR|) = 1/4(|HH\rangle\langle HH| + |HV\rangle\langle HV| + |VH\rangle\langle VH| + |VV\rangle\langle VV| + |HH\rangle\langle VV| + |VV\rangle\langle HH| - |HV\rangle\langle VH| - |VH\rangle\langle HV|)$. In figure 5 a preliminary result is shown, where the temporal delay between both sources is changed while counting HH coincidences between modes a and c triggered on the detection of a right circularly polarized photon in mode T*. A coherent overlap is indicated by the increase of the triggered HH count rate. A Gaussian fit gives a visibility of $(46.1 \pm 4.0)\%$, whereas ideally 100% are expected. This reduced visibility will be a matter of further investigation. However, the principle feasibility of coherently overlapping the WCB and the SPDC emission as a first step in the presented experimental setup is demonstrated. The next step will be the proof of observing GHZ_4^- and W_4 entangled states with this setup.

4. SUMMARY

We have demonstrated that it is possible to construct photon sources based on linear optics that allow to prepare a variety of qualitatively different quantum states by using the higher dimensional Hilbert space opened via an additional photon. Local manipulations suffice to obtain the different kinds of entanglement that can otherwise not be transformed into each other by local operations. Hence, we were able to demonstrate experimentally the observation of states from both inequivalent classes of genuine tripartite entanglement via a simple projection measurement on a single four-photon entangled state. Further, we extended this approach to achieve different, inequivalent and highly relevant four-photon entangled states starting from five-photon entangled states, all realizable in a single linear optics setup by simple local operations. The latter demonstrates the flexibility of

*First order interference is not observed for the examined coincidence as no other possibility exists how to observe a triggered HH coincidence. The observed coherence length is $(120 \pm 11)\mu$m.

this experimental linear optics approach in observing a multitude of quantum states, whereas most linear optics setups are restricted to the observation of only a single quantum state.

ACKNOWLEDGMENTS

We acknowledge the support of this work by Deutsche Forschungsgemeinschaft through the DFG-Cluster of Excellence "Munich Centre for Advanced Photonics" (www.munich-photonics.de) and the European Commission through the EU Project QAP. We further acknowledge a fruitful collaboration with G. Tóth and E. Solano. W.W. acknowledges support by QCCC of the Elite Network of Bavaria and the Studienstiftung des deutschen Volkes.

REFERENCES

1. C. H. Bennett, S. Popescu, D. Rohrlich, J. A. Smolin, and A. V. Thapliyal, "Exact and asymptotic measures of multipartite pure-state entanglement," *Phys. Rev. A* **63**, p. 012307, Dec 2000.
2. W. Dür, G. Vidal, and J. I. Cirac, "Three qubits can be entangled in two inequivalent ways," *Phys. Rev. A* **62**, p. 062314, Nov 2000.
3. F. Verstraete, J. Dehaene, B. D. Moor, and H. Verschelde, "Four qubits can be entangled in nine different ways," *Phys. Rev. A* **65**(5), p. 052112, 2002.
4. L. Lamata, J. Leon, D. Salgado, and E. Solano, "Inductive classification of multipartite entanglement under stochastic local operations and classical communication," *Phys. Rev. A* **74**(5), p. 052336, 2006.
5. L. Lamata, J. Leon, D. Salgado, and E. Solano, "Inductive entanglement classification of four qubits under stochastic local operations and classical communication," *Phys. Rev. A* **75**(2), p. 022318, 2007.
6. M. Eibl, S. Gaertner, M. Bourennane, C. Kurtsiefer, M. Żukowski, and H. Weinfurter, "Experimental observation of four-photon entanglement from parametric down-conversion," *Phys. Rev. Lett.* **90**(20), p. 200403, 2003.
7. M. Eibl, N. Kiesel, M. Bourennane, C. Kurtsiefer, and H. Weinfurter, "Experimental realization of a three-qubit entangled w state," *Phys. Rev. Lett.* **92**(7), p. 077901, 2004.
8. H. Mikami, Y. Li, K. Fukuoka, and T. Kobayashi, "New high-efficiency source of a three-photon w state and its full characterization using quantum state tomography," *Phys. Rev. Lett.* **95**(15), p. 150404, 2005.
9. N. Kiesel, C. Schmid, U. Weber, G. Tóth, O. Gühne, R. Ursin, and H. Weinfurter, "Experimental analysis of a four-qubit photon cluster state," *Phys. Rev. Lett.* **95**(21), p. 210502, 2005.
10. P. Walther, K. J. Resch, T. Rudolph, E. Schenck, H. Weinfurter, V. Vedral, M. Aspelmeyer, and A. Zeilinger, "Experimental one-way quantum computing," *Nature* **434**(7030), pp. 169–176, 2005.
11. N. Kiesel, C. Schmid, G. Tóth, E. Solano, and H. Weinfurter, "Experimental observation of four-photon entangled dicke state with high fidelity," *Phys. Rev. Lett.* **98**(6), p. 063604, 2007.
12. A. Sen(De), U. Sen, M. Wieśniak, D. Kaszlikowski, and M. Żukowski, "Multiqubit w states lead to stronger nonclassicality than greenberger-horne-zeilinger states," *Phys. Rev. A* **68**, p. 062306, Dec 2003.
13. R. H. Dicke, "Coherence in spontaneous radiation processes," *Phys. Rev.* **93**(1), pp. 99–110, 1954.
14. J. K. Stockton, J. M. Geremia, A. C. Doherty, and H. Mabuchi, "Characterizing the entanglement of symmetric many-particle spin-(1/2) systems," *Phys. Rev. A* **67**(2), p. 022112, 2003.
15. T. Yamamoto, K. Tamaki, M. Koashi, and N. Imoto, "Polarization-entangled w state using parametric down-conversion," *Phys. Rev. A* **66**, p. 064301, Dec 2002.
16. M. Bourennane, M. Eibl, C. Kurtsiefer, S. Gaertner, H. Weinfurter, O. Gühne, P. Hyllus, D. Bruss, M. Lewenstein, and A. Sanpera, "Experimental detection of multipartite entanglement using witness operators," *Phys. Rev. Lett.* **92**(8), p. 087902, 2004.
17. A. Zeilinger, M. A. Horne, H. Weinfurter, and M. Żukowski, "Three-particle entanglement from two entangled pairs," *Phys. Rev. Lett.* **78**(16), pp. 3031–3034, 1997.
18. J.-W. Pan, M. Daniell, S. Gasparoni, G. Weihs, and A. Zeilinger, "Experimental demonstration of four-photon entanglement and high-fidelity teleportation," *Phys. Rev. Lett.* **86**(20), pp. 4435–4438, 2001.

19. N. K. Langford, T. J. Weinhold, R. Prevedel, K. J. Resch, A. Gilchrist, J. L. O'Brien, G. J. Pryde, and A. G. White, "Demonstration of a simple entangling optical gate and its use in bell-state analysis," *Phys. Rev. Lett.* **95**(21), p. 210504, 2005.
20. N. Kiesel, C. Schmid, U. Weber, R. Ursin, and H. Weinfurter, "Linear optics controlled-phase gate made simple," *Phys. Rev. Lett.* **95**(21), p. 210505, 2005.
21. R. Okamoto, H. F. Hofmann, S. Takeuchi, and K. Sasaki, "Demonstration of an optical quantum controlled-not gate without path interference," *Phys. Rev. Lett.* **95**(21), p. 210506, 2005.
22. W. Dür and J. I. Cirac, "Multiparticle entanglement and its experimental detection," *J. Phys. A* **34**(35), pp. 6837–6850, 2001.
23. H. Häffner, W. Hansel, C. F. Roos, J. Benhelm, D. Chek-al kar, M. Chwalla, T. Korber, U. D. Rapol, M. Riebe, P. O. Schmidt, C. Becher, O. Gühne, W. Dur, and R. Blatt, "Scalable multiparticle entanglement of trapped ions," *Nature* **438**, pp. 643–646, Dec. 2005.
24. I. Ghiu, M. Bourennane, and A. Karlsson, "Entanglement-assisted local transformations between inequivalent classes of three-particle entangled states," *Phys. Lett. A* **287**(1-2), pp. 12–18, 2001.
25. J. G. Rarity and P. R. Tapster, "Three-particle entanglement from entangled photon pairs and a weak coherent state," *Phys. Rev. A* **59**(1), pp. R35–R38, 1999.